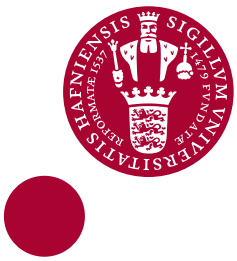

PKD Phosphorylation as Novel Pathway of KV11.1 Regulation

Steffensen, Annette Buur; Bomholtz, Sofia Hammami; Andersen, Martin Nybo; Olsen, Jesper Velgaard; Mutsaers, N.; Lundegaard, Pia Rengtved; Lundby, Alicia; Schmitt, Nicole

Published in:
Cellular Physiology and Biochemistry

DOI:
10.1159/000491007

Publication date:
2018

Document version
Publisher's PDF, also known as Version of record

Cellular Physiology and Biochemistry

Cell Physiol Biochem 2018;47:1742-1750
DOI: 10.1159/000491007
Published online: June 28, 2018
Accepted: March 23, 2018

Original Paper

PKD Phosphorylation as Novel Pathway of K_V11.1 Regulation

Annette Buur Steffensen[a] Sofia Hammami Bomholtz[a] Martin Nybo Andersen[a] Jesper Velgaard Olsen[b] Nancy Mutsaers[a] Pia Rengtved Lundegaard[a] Alicia Lundby[a,b] Nicole Schmitt[a]

[a]Danish National Research Foundation Centre for Cardiac Arrhythmia and Dept. of Biomedical Sciences, Faculty of Health and Medical Sciences, University of Copenhagen, Copenhagen, [b]Novo Nordisk Foundation Center for Protein Research, Department for Proteomics, Faculty of Health and Medical Sciences, University of Copenhagen, Copenhagen, Denmark

Key Words
K_V11.1 • HERG • Phosphorylation • Protein kinase • PKD • Mass spectrometry • Patch-clamp electrophysiology

Abstract
Background/Aims: The voltage-gated potassium channel K_V11.1 has been originally cloned from the brain and is expressed in a variety of tissues. The role of phosphorylation for channel function is a matter of debate. In this study, we aimed to elucidate the extent and role of protein kinase D mediated phosphorylation. ***Methods:*** We employed mass spectrometry, whole-cell patch clamp electrophysiology, confocal microscopy, site-directed mutagenesis, and western blotting. ***Results:*** Using brain tissue from rat and mouse, we mapped several phosphorylated K_V11.1 residues by LC-MS mass spectrometry and identified protein kinase D (PKD1) as possible regulatory kinase. Co-expression of K_V11.1 with PKD1 reduced current amplitudes without altering protein levels or surface expression of the channel. Based on LC-MS results from *in vivo* and HEK293 cell experiments we chose four K_V11.1 mutant candidates for further functional analysis. Ablation of the putative PKD phosphorylation site in the mutant S284A increased the maximal current indicating S284 as a main PKD target in K_V11.1. ***Conclusions:*** Our data might help mitigating a long-standing controversy in the field regarding PKC regulation of K_V11.1. We propose that PKD1 mediates the PKC effects on K_V11.1 and we found that PKD targets S284 in the N-terminus of the channel.

Introduction

The potassium channel K_V11.1 is encoded by *KCNH2* and also known as human-ether-a-go-go related gene type 1 (hERG). The tetrameric channel protein is expressed in a variety

A. Lundby and N. Schmitt contributed equally to this work.

Nicole Schmitt
Danish National Research Foundation Centre for Cardiac Arrhythmia and Dept. of Biomedical Sciences Faculty of Health and Medical Sciences, Mærsk Tower 07-9-36, Blegdamsvej 3, 2200 Copenhagen N (Denmark); Tel. +45 35327448; Fax +45 35327555; E-Mail nschmitt@sund.ku.dk

of tissues including brain, heart, pancreas, vasculature, and a number of tumors [1]. It is best known for its role in the heart, where it is the molecular correlate of the rapid delayed rectifying current I_{Kr} [2, 3]. Mutations in the *KCNH2* gene are associated with several cardiac arrhythmias such as Long QT and Short QT syndromes and atrial fibrillation [1, 2, 4].

Several posttranscriptional and posttranslational mechanisms have been described to finetune expression levels and/or biophysical parameters of K_V11.1 [5–7]. Protein kinase A (PKA) phosphorylates K_V11.1 directly at four consensus sites *in vitro* [8, 9]. Protein kinase C (PKC) effects have been investigated in different expression systems and experimental models (reviewed in [1]). Despite numerous studies, it is still unresolved whether PKC directly phosphorylates the channel protein. Identification of 18 consensus sites by prediction algorithms and individual ablation of these sites did not provide any evidence for a direct phosphorylation at these sites [10, 11]. Cockerill et al. provided evidence for a role of the channel's N-terminus for PKC mediated phosphorylation [11]. It has been suggested that an atypical PKC phosphorylation site might be involved in the PKC effects [1, 11].

Noteworthy, multiple lines of evidence indicate that PKC activity is indispensable for activation of protein kinase D (PKD). Especially, the novel PKCs Ɛ and η give robust activation of PKD [12] but also classical PKCα can activate PKD [13]. PKD is expressed in a variety of tissues and its function has been implicated in health and disease (reviewed in [14–16]). Several studies found that a variety of stimuli induce PKD activation through the α-adrenergic pathway, and in many cases this could be attenuated by PKC inhibition [17–19]. Here, we hypothesized that PKC effects on K_V11.1 are mediated through PKD1.

Materials and Methods

Protein biochemistry

Preparation of brain samples. All procedures involving animals conformed to Danish animal welfare regulations. Briefly, mouse or rat brain was cut in smaller pieces, homogenized in buffer [in mM: 50 Tris/HCl pH 7.4, 2.5 EGTA, 5 EDTA, 10 NaCl, 10 KCl, 0.5 pefabloc, 0.1 NaF, and 320 sucrose with a protease inhibitor cocktail (in μg/mL: 2 aprotinin, 1 leupeptin, 2 antipain, 10 benzamidine, and one tablet of phosSTOP/10 mL)] and centrifuged. The supernatant was retained, centrifuged again, and pellets were resuspendend in 2.5 mL homogenizing buffer for every gram of brain.

Preparation of HEK293 cell samples. HEK293 cells were transfected with K_V11.1 alone or co-expressed with PKD1. For mass spectrometry the cells were grown in a special media, immunoprecipitated and digested to peptides. For lysates cells were harvested in solubilization buffer without detergent [in mM: 50 Tris pH 8.5, 150 NaCl, 5 EDTA] and supplemented with 8 μM leupeptin, 0.4 mM pefabloc and one tablet of phosSTOP pr. 10 mL, centrifuged (2 min, 100 x g) and incubated with solubilization buffer containing 1% NP-40 on a spinning wheel for 3 hours. Samples were centrifuged at >10.000 x g for 10 min and supernatants were aliquoted, frozen in liquid nitrogen and stored until further use.

Sample preparation for mass spectrometry. Sample lysates were precleared with Protein G-dynabeads (Invitrogen). Then primary antibody (2 μg/1 mg total protein in the sample) was added followed by overnight incubation. After addition of dynabeads in lysis buffer [in mM: 50 Tris/HCl, pH 8.5, 5 EDTA, 150 NaCl] containing 1% NP-40, 8 μM leupeptin (Sigma), 0.4 mM pefabloc (Sigma), one tablet of phosSTOP pr. 10 mL (Roche) and incubation for 2 h, multiple wash steps were performed. At the end beads were resuspended in Laemmli buffer (containing 100 mM DTT) and incubated for 3 min at 70°C.

Mass spectrometry. Immunoprecipitated proteins were separated by SDS-PAGE, fixed, stained, bands excised and proteins proteolytically cleaved to peptides as previously described [20, 21]. Peptide separation was performed by reversed-phase C_{18} HPLC on an Easy nLC system (Thermo Fisher Scientific). The effluent from the HPLC was directly electrosprayed into an LTQ Orbitrap Velos mass spectrometer (Thermo Fisher Scientific, Slangerup, Denmark) through a nano-spray ion source. The peptide mixture was analyzed by full-scan MS spectra (*m/z* 300-2000, resolution 30, 000) in the Orbitrap analyzer. For every full-scan the

most intense peptide ions were sequentially isolated, fragmented by higher energy collisional dissociation (HCD), and fragments were recorded by the Orbitrap mass analyzer. The acquired data was processed by MaxQuant (version 1.1.1.25) (Max-Planck Institute of Biochemistry, Department of Proteomics and Signal Transduction, Munich, Germany).

Patch-clamp electrophysiology

Recordings. All recordings of transiently transfected HEK293 cells were performed in the whole-cell patch clamp configuration using an EPC9 patch clamp amplifier (HEKA Elektronik, Lambrecht, Germany). Data acquisition was done with the Pulse software (HEKA Electronik). The series resistance recorded in the whole cell configuration was kept below 10 MΩ and compensated (80%). The extracellular solution contained [in mM: 140 NaCl, 4 KCl, 2 $CaCl_2$, 1 $MgCl_2$, and 10 HEPES, pH=7.4]. The intracellular solution contained [in mM: 110 KCl, 10 EGTA, 5.17 $CaCl_2$, 1.42 $MgCl_2$, 4 K_2ATP, and 10 HEPES, pH=7.2]

Protocols. Current–voltage (I/V) relations were obtained from the step-protocol by plotting the outward current at the end of the 1-second test pulse as a function of the test potential. The voltage-dependence of activation was determined by fitting the amplitude of peak tail currents versus test potential to a two-state Boltzmann distribution of the form $I(V) = 1/(1+\exp[(V_{½} - V)/a])$, where $V_{½}$ = potential for half-maximal activation, and a = slope factor. Other kinetic parametres were analysed as described in detail (for all online suppl. material, see www.karger.com/doi/10.1159/000491007) in the Supplementary Methods.

Data analysis. Data analysis was performed using Excel (Microsoft), Igor Pro 4.04 (Wavemetrics, OR, USA) and Prism 4 (GraphPad Software, CA, USA). All values are given as mean ± SEM. The number of independent experiments is indicated by n. Statistical comparisons of results were performed using one-way analysis of variance (ANOVA) or two-way ANOVA. Following ANOVA, Bonferroni's method of multiple comparisons was used to identify significant differences between means. A value of $P < 0.05$ was considered statistically significant.

Antibodies

Primary antibodies: anti-K_V11.1, APC-062 (Alomone, Jerusalem, Israel, 1:500); anti-PKD1, H00005587-A01 (Abnova, Roskilde, Denmark, 1:500); anti-β-tubulin, MAB3408 (Millipore, Hellerup, Denmark, 1:4000).

Secondary antibodies: For western blot analyses; peroxidase conjugated affinipure F(ab)fragment donkey anti-rabbit and anti-mouse (Jackson ImmunoResearch, Suffolk, UK), donkey anti-mouse 680RD, 926-68072 (LI-COR Biosciences, Copenhagen, Denmark); goat anti-rabbit 800CW, 926-32211 (LI-COR Biosciences). For confocal imaging; Alexa Fluor®488-conjugated donkey anti-rabbit IgG (1:200), Alexa Fluor®568-conjugated donkey anti-mouse IgG (1:200). Alexa®Fluor 647 Phalloidin (1:200) was used to stain actin filaments and DAPI (1:300) was used to stain the nucleus. Secondary antibodies were purchased from Invitrogen (Glostrup, Denmark).

Molecular biology

Point mutations in K_V11.1 (GenBank Acc. No. NM_000238) were introduced by standard site-directed mutagenesis. All constructs were verified by complete DNA sequencing of the cDNA insert (Macrogen Inc., Seoul, Rep. of Korea). Human protein kinase D1 (PKD1, NM_002742) expression plasmid was kindly provided by Dr. A. Hausser (University of Stuttgart, Germany) [22].

Results

K_V11.1 is phosphorylated in vivo at a residue matching a consensus recognition site for PKD

First, we mapped the *in vivo* phosphorylation sites of K_V11.1 using tissue samples, where K_V11.1 channels from both mouse and rat brain tissue were purified by immunoprecipitations and submitted to analysis by LC-MS/MS mass spectrometry. Our analysis led to identification of 14 *in-vivo* phosphorylation sites (Table 1). In Table 1 we assigned the identified residues

from mouse and rat to the nomenclature of the human K_V11.1 residues by alignment of mouse, rat, and human sequences (see online suppl. material, Suppl. Fig. S1). Our data confirmed phosphorylation at residue S283 which had been reported as a site for PKA-mediated phosphorylation previously [9]. None of the identified residues were PKC consensus sites; however, S284 was a strong candidate for PKD phosphorylation.

Table 1. Phosphosites in mouse and rat tissue and HEK293 cells determined by LC-MS/MS. Numbering based on human sequence (in italics corresponding residue in rat or mouse, respectively). Best motif is predicted by MaxQuant [38].

tissue		HEK293	best motif
rat brain	mouse brain		
-	S140		ERK/MAPK
S239 (*S241*)	S239 (*S241*)		ERK/MAPK
S250 (*S252*)	-		CDK1
-	-	S263	
-	-	S266	
S283 (*S285*)	-		PKA
S284 (*S286*)	-	S284	PKD
S304 (*S306*)	-		CamKII
T319 (*T321*)	-	T319	NEK6
	S320 *(S322)*	S320	
-	S322 (*S324*)	S322	CK1
-	S351 (*S353*)		Proline-directed
-	T353 (*T355*)	T353	
-	S871 (*S873*)		ERK/MAPK
-	S874 (*S876*)		CK1
S969 (*S971*)	-		

Co-expression of PKD1 reduces K_V11.1 current densities

We assessed a possible role of PKD1 by employing whole-cell patch clamp recordings. We transiently transfected HEK293 cells with K_V11.1 alone or co-expressed with PKD1 cDNA (Fig. 1). To investigate the potassium currents, we applied a standard step protocol with 1 s test pulses ranging from -100 to +60 mV in 10 mV increments. Fig. 1A shows representative current recordings of K_V11.1 and K_V11.1 + PKD1. As expected, the current/voltage relationship (IV curve) resulted in the characteristic bell-shape due to inactivation of the channel [3]. Of note, a high degree of cell to cell variability of current levels was seen in line with literature [23]. The maximum outward current amplitude was normalized to the cell capacitance and used to construct the current-voltage (I-V) relationship of K_V11.1 (n=7) and K_V11.1 co-expressed with PKD1 (n=7) (Fig. 1B). The maximum outward current amplitude at +20 mV for K_V11.1 was 29.5±9.5 pA/pF and significantly reduced by 56.2 % upon co-expression with PKD1 (12.9±1.7 pA/pF, P=0.018).

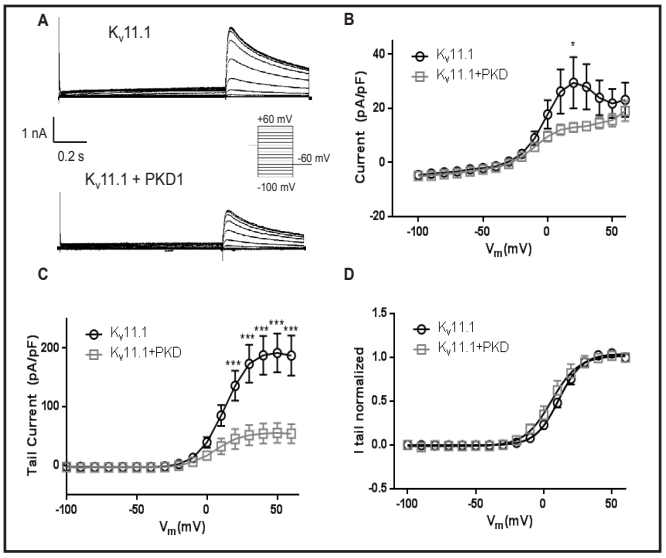

Fig. 1. Co-expression of PKD1 reduces K_V11.1 current amplitudes. A. Representative current recordings of K_V11.1 and K_V11.1+PKD1 from transiently transfected HEK293 cells. The insert depicts the voltage clamp protocol. B. Currents measured at the end of each step were used to construct the current-voltage (IV) relationship. C. Tail currents and D. normalized tail currents measured at -60 mV. The solid lines correspond to the fitted Boltzmann functions. K_V11.1 (n=7) and K_V11.11+PKD (n=7). *P<0.05, **P<0.01, ***<0.001.

The tail current amplitude was also reduced by PKD1 co-expression (Fig. 1C). K_V11.1 current reduction has earlier been assigned to a shift of the voltage-dependent activation to more depolarized potentials [24]. Therefore, the normalized peak tail currents were fitted to a Boltzmann function to determine the $V_{½}$ values of voltage-dependent activation. No difference of the voltage-dependent activation upon co-expression of PKD1 (Fig. 1D, Table 2) was observed. Deactivation, inactivation and recovery from inactivation properties (Table 2) were unchanged.

Table 2. Effect of PKD1 co-expression on the biophysical properties of K_V11.1. *P<0.05

	Kv11.1 (n = 7)	Kv11.1 + PKD (n = 7)
Activation		
Maximum outward current (at +20 mV) (pA/pF)	29.5±9.5	12.9±1.7*
$V_{½}$ (mV)	11.77±1.6	7.6 ± 3.7
Slope (mV)	8.66±0.5	8.9± 0.9
Recovery from inactivation		
$V_{½}$ (mV)	-78.1±3.1	-74.1±2.3
Slope (mV)	19.3±0.9	21.5±3.2
τ_{rec} at -60 mV (ms)	6.2±0.8	5.5±0.4
Deactivation		
τ_{slow} at -60 mV (ms)	993.3±102	849.9±48.7
τ_{fast} at -60 mV (ms)	130.2±8.3	103.2± 19.9
$A_{fast}/(A_{fast}+A_{slow})$ at -60 mV	0.3±0.01	0.26±0.02
Inactivation		
τ_{Inact} at 0 mV (ms)	6.2±0.4	5.8±0.4

PKD1 co-expression does not alter protein levels or surface expression of Kv11.1

We assessed whether PKD1 co-expression would affect K_V11.1 protein expression or subcellular localization. Western blot experiments revealed that there was no change in protein levels (see online suppl. material, Suppl. Fig. S2). PKD1 did not alter the localization of K_V11.1 in HEK293 cells, and K_V11.1 and PKD1 were both localized in the plasma membrane as assessed by confocal microscopy (see online suppl. material, Suppl. Fig. S3). Attempts to test a possible direct interaction between K_V11.1 channel and PKD1 by co-immunoprecipitation remained unsuccessful (data not shown).

PKD1 co-expression leads to K_V11.1 phosphorylation in HEK293 cells

To analyse whether S284 and other residues would be phosphorylated by PKD1, we immunoprecipitated K_V11.1 channels co-expressed with PKD1 in HEK293 cells to map the phosphorylation sites by mass spectrometry. We identified seven residues that were phosphorylated upon co-expression with PKD1. This indicated that PKD1 could affect K_V11.1 phosphorylation in a heterologous expression system by direct phosphorylation of several residues. MS/MS spectra for all identified sites with evidence for site localization are provided (see online suppl. material) in Suppl. Fig. S4-9. A few residues did stand out from the data; Residue S284 appeared to be phosphorylated in HEK293 cells co-expressed with PKD1. In addition, it was identified *in vivo* and motif-wise PKD1 was the most likely kinase to phosphorylate this site, making S284 our prime candidate for PKD1 phosphorylation. Also amino acids S263 and S266 were phosphorylated. S266 was identified to be phosphorylated by itself, whereas S263 was only identified in peptides where S266 was also phosphorylated and we decided to address their combined effect in the subsequent functional analysis. S322 was phosphorylated and found in a cluster together with S318, T319, and S320. Three of the four were found phosphorylated *in vivo*. We chose to address the combined effects of the four residues in the cluster. Finally, residue T353 appeared to be phosphorylated in HEK293 cells and *in vivo*.

Functional analysis of K_V11.1 mutants supports S284 as possible PKD target

We sought to address the functional impact of the selected amino acids after ablation of the serine residues to alanine (A) hereby mimicking the dephosphorylated state. To this end, we generated four K_V11.1 mutants (K_V11.1-S284A, K_V11.1-S263/S266A, K_V11.1-S318/

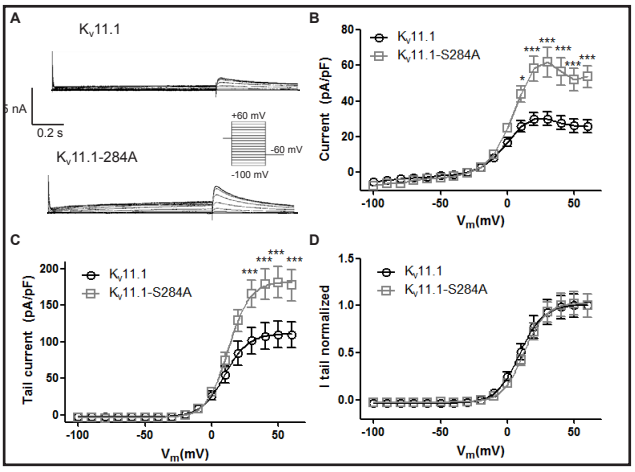

Fig. 2. Ablation of phosphorylation site S284 increases K_V11.1 mediated currents. A. Representative current recordings of K_V11.1-WT and K_V11.1-S284A from transiently transfected HEK293 cells. The insert shows the voltage clamp protocol. B. Currents measured at the end of each step were used to construct the current-voltage (IV) relationship. C. Tail currents and D. normalized tail currents measured at -60 mV. The solid lines correspond to the fitted Boltzmann functions. K_V11.1 (n=8) and K_V11.1-S284A (n=11). *P<0.05, ***P<0.001.

T319/S320/S322A, and K_V11.1-T353A). We expressed the mutant channels in HEK293 and analysed biophysical parameters by patch-clamp electrophysiology.

K_V11.1-S284A displayed a significantly higher maximum outward current amplitude than wild-type K_V11.1 at +20 mV; S284A: 58.2±6.9 (n=11), WT: 29.9±3.5 pA/pF (n=8, P<0.001) respectively; (Fig. 2A,B) indicating that this residue mediates at least some of the PKD1 phosphorylation effect on the channel. Also the tail current amplitude was significantly higher for the mutant (Fig. 2C). We did not observe any significant shift in the voltage-dependent activation for K_V11.1-S284A compared with wild-type (Fig. 2D, Table 3). The slow time constant of deactivation was significantly faster at -60 and -50 mV for the S284A mutant compared to wild-type. Other voltage-dependent and kinetic parameters were unaffected by the alanine mutation (Table 3). We analysed protein levels of S284A by western blotting experiments and found that expression levels were similar to wild-type channels (see online suppl. material, Suppl. Fig. S2). K_V11.1-S263/S266A, K_V11.1-S318/T319/S320/S322A, and K_V11.1-T353A behaved similarly to wild-type channels (see online suppl. material, Suppl. Table S1).

Table 3. Effect of S284 ablation on biophysical parameters. **P<0.01, ***P<0.001

	Kv11.1-WT (n = 8)	Kv11.1-S284A (n = 11)
Activation		
Maximum outward current (at +20 mV) (pA/pF)	29.9±3.5	58.2±6.9***
$V_{½}$ (mV)	10.2 ± 2.1	11.7 ± 1.3
Slope (mV) (at + 20 mV)	8.6 ± 0.2	7.8 ± 0.2
Recovery from inactivation		
$V_{½}$ (mV)	-75.5 ± 1.8	-71.8 ± 1.2
Slope (mV)	15.9 ± 0.5	16.7 ± 0.2
τ_{rec} at -60 mV (ms)	4.1 ± 0.4	3.8 ± 0.2
Deactivation		
τ_{slow} at -60 mV (ms)	1010.8 ± 49.7	779.9 ± 38.5**
τ_{fast} at -60 mV (ms)	125.8 ± 5.9	114.5 ± 2.7
$A_{fast}/(A_{fast}+A_{slow})$ at -60 mV	0.3 ± 0.02	0.3 ± 0.02
Inactivation		
τ_{Inact} at 0 mV (ms)	7.2 ± 0.7	7.6 ± 0.4

Discussion

K_V11.1 is an important potassium channel which is manifested in its association with inherited and acquired cardiac arrhythmia where even mild changes of the conducted current

may have deleterious effects. The current conducted by K_V11.1 is regulated by a number of physiological stimuli mediated by G-protein coupled receptors, e.g. α- and β-adrenergic, muscarinic, and angiotensin II receptors [11, 25–29]. Hence, understanding the molecular basis of the regulation is crucial for elucidating disease mechanisms [1, 30]. Here, we provide evidence for involvement of protein kinase D based on *in vivo* and *in vitro* mass-spectrometry findings together with functional analysis of wild-type and mutant K_V11.1 channels.

LC-MS mass spectrometry revealed several phosphorylated residues *in vivo* and suggested PKD as a strong candidate. Co-expression of K_V11.1 with PKD1 reduced current amplitudes; however, we were unable to identify significant changes in kinetic parameters that could explain the decrease in I_{max}. Protein levels were unaffected. Due to the lack of specific pharmacological tools, i.e. specific activators or blockers of PKD1 which would allow for an assessment of PKD1 effects independent of PKC in patch-clamp recordings [14], we instead chose four candidate K_V11.1 mutants for further functional analysis based on the results obtained from HEK293 cell experiments and *in vivo* data. Ablation of the putative PKD phosphorylation site in the mutant S284A increased the maximal current.

Our data might help mitigating a long-standing controversy in the field regarding PKC regulation of the channel. Most studies have investigated the acute effects of different pathways upstream of PKC activation with variable results ranging from reports indicating that neither PKC nor PKA are involved [31], that PKA and PKC show composite and partial effects with complex cross-talk [32], or that either convential PKC (cPKC) [10] or novel PKC (nPKC) [25] are exclusively involved. Other pivotal points of discussion have been whether PKC phosphorylates the channel directly [10, 11, 27] and whether PKC mediated phosphorylation increases [32] or decreases current K_V11.1 (or I_{Kr}) amplitudes [10, 11, 24, 26, 27]. However, the majority of studies found a positive shift in the voltage-dependence of activation and an acceleration of deactivation, with different levels of reduction of the K_V11.1 current amplitude (e.g [10, 11, 27, 33].)

Our results support the notion that PKC mediated functional effects are independent of the previously suggested consensus sites [10]. They also confirm a role of the N-terminal part of the protein as proposed by other studies [11, 34]. Cockerill and coworkers found that residues 2-354 of the K_V11.1 N-terminus are critical for both cPKC phosphorylation and functional modulation of the channel [11]. Of note, both cPKC [13] and nPKC [12] have been reported to activate PKD1. While we cannot rule out that PKC exerts a variety of direct and indirect effects, we propose that PKD1 is a new player, either activated independently or downstream of PKC, targeting S284 in the N-terminus of the channel.

Recent attempts to resolve the identity of the involved PKC isoform by using inhibitory peptidomimmetics indicated a predominant role of PKCε, with minor contributions of PKCβ, PKCα, and PKCη [35]. Interestingly, Haworth and coworkers reported that in adult cardiomyocytes PKCε is the predominant activator of PKD and this activation was somewhat counteracted by PKA activation indicating a crosstalk between the two kinase pathways [18]. This crosstalk might mainly be a PKC effect on the cAMP level [36, 37], but the molecular mechanism behind this is currently unclear. Therefore, we did not investigate the candidates that are already known to be phosphorylated by PKA.

Conclusion

Our data indicate that PKD1 contributes to K_V11.1 regulation by targeting S284 in the N-terminus of the channel. This pathway could therefore present an explanation to years of divergent results regarding the regulation of I_{Kr} or K_V11.1 by protein kinases.

Acknowledgements

This work was supported by the Danish National Research Foundation.

Disclosure Statement

The authors declare to have no conflict of interests.

References

1 Vandenberg JI, Perry MD, Perrin MJ, Mann SA, Ke Y, Hill AP: hERG K(+) channels: structure, function, and clinical significance. Physiol Rev 2012;92:1393–1478.
2 Sanguinetti MC, Tristani-Firouzi M: hERG potassium channels and cardiac arrhythmia. Nature 2006;440:463–469.
3 Sanguinetti MC, Jiang C, Curran ME, Keating MT: A mechanistic link between an inherited and an acquired cardiac arrhythmia: HERG encodes the IKr potassium channel. Cell 1995;81:299–307.
4 Hong K, Bjerregaard P, Gussak I, Brugada R: Short QT syndrome and atrial fibrillation caused by mutation in KCNH2 J Cardiovasc Electrophysiol 2005;16:394–396.
5 Gong Q, Zhang L, Vincent GM, Horne BD, Zhou Z: Nonsense mutations in hERG cause a decrease in mutant mRNA transcripts by nonsense-mediated mRNA decay in human long-QT syndrome. Circulation 2007;116:17–24.
6 Albesa M, Grilo LS, Gavillet B, Abriel H: Nedd4-2-dependent ubiquitylation and regulation of the cardiac potassium channel hERG1 J Mol Cell Cardiol 2011;51:90–98.
7 Petrecca K, Atanasiu R, Akhavan A, Shrier A: N-linked glycosylation sites determine HERG channel surface membrane expression. J Physiol 1999;515 (Pt 1):41–48.
8 Cui B, Zhu X, Xu M, Guo T, Zhu D, Chen G, Li X, Xu L, Bi Y, Chen Y, Xu Y, Li X, Wang W, Wang H, Huang W, Ning G: A genome-wide association study confirms previously reported loci for type 2 diabetes in Han Chinese. PloS One 2011;6:e22353.
9 Thomas D, Zhang W, Karle CA, Kathöfer S, Schöls W, Kübler W, Kiehn J: Deletion of protein kinase A phosphorylation sites in the HERG potassium channel inhibits activation shift by protein kinase A. J Biol Chem 1999;274:27457–27462.
10 Thomas D, Zhang W, Wu K, Wimmer AB, Gut B, Wendt-Nordahl G, Kathöfer S, Kreye VA, Katus HA, Schoels W, Kiehn J, Karle CA: Regulation of HERG potassium channel activation by protein kinase C independent of direct phosphorylation of the channel protein. Cardiovasc Res 2003;59:14–26.
11 Cockerill SL, Tobin AB, Torrecilla I, Willars GB, Standen NB, Mitcheson JS: Modulation of hERG potassium currents in HEK-293 cells by protein kinase C. Evidence for direct phosphorylation of pore forming subunits. J Physiol 2007;581:479–493.
12 Zugaza JL, Sinnett-Smith J, Van Lint J, Rozengurt E: Protein kinase D (PKD) activation in intact cells through a protein kinase C-dependent signal transduction pathway. EMBO J 1996;15:6220–6230.
13 Wong C, Jin Z-G: Protein kinase C-dependent protein kinase D activation modulates ERK signal pathway and endothelial cell proliferation by vascular endothelial growth factor. J Biol Chem 2005;280:33262–33269.
14 Avkiran M, Rowland AJ, Cuello F, Haworth RS: Protein kinase d in the cardiovascular system: emerging roles in health and disease. Circ Res 2008;102:157–163.
15 Ellwanger K, Hausser A: Physiological functions of protein kinase D in vivo. IUBMB Life 2013;65:98–107.
16 Haworth RS, Goss MW, Rozengurt E, Avkiran M: Expression and activity of protein kinase D/protein kinase C mu in myocardium: evidence for alpha1-adrenergic receptor- and protein kinase C-mediated regulation. J Mol Cell Cardiol 2000;32:1013–1023.
17 Harrison BC, Kim M-S, van Rooij E, Plato CF, Papst PJ, Vega RB, McAnally JA, Richardson JA, Bassel-Duby R, Olson EN, McKinsey TA: Regulation of cardiac stress signaling by protein kinase d1. Mol Cell Biol 2006;26:3875–3888.
18 Haworth RS, Roberts NA, Cuello F, Avkiran M: Regulation of protein kinase D activity in adult myocardium: novel counter-regulatory roles for protein kinase Cepsilon and protein kinase A. J Mol Cell Cardiol 2007;43:686–695.
19 Roberts NA, Haworth RS, Avkiran M: Effects of bisindolylmaleimide PKC inhibitors on p90RSK activity in vitro and in adult ventricular myocytes. Br J Pharmacol 2005;145:477–489.

20 Lundby A, Olsen JV: GeLCMS for in-depth protein characterization and advanced analysis of proteomes. Methods Mol Biol Clifton NJ 2011;753:143–155.
21 Lundby A, Rossin EJ, Steffensen AB, Acha MR, Newton-Cheh C, Pfeufer A, Lynch SN; QT Interval International GWAS Consortium (QT-IGC), Olesen SP, Brunak S, Ellinor PT, Jukema JW, Trompet S, Ford I, Macfarlane PW, Krijthe BP, Hofman A, Uitterlinden AG, Stricker BH, Nathoe HM, Spiering W, Daly MJ, Asselbergs FW, van der Harst P, Milan DJ, de Bakker PI, Lage K, Olsen JV: Annotation of loci from genome-wide association studies using tissue-specific quantitative interaction proteomics. Nat Methods 2014;11:868–874.
22 Hausser A, Link G, Bamberg L, Burzlaff A, Lutz S, Pfizenmaier K, Johannes FJ: Structural requirements for localization and activation of protein kinase C mu (PKC mu) at the Golgi compartment. J Cell Biol 2002;156:65–74.
23 Larsen AP, Olesen S-P: Differential expression of hERG1 channel isoforms reproduces properties of native I(Kr) and modulates cardiac action potential characteristics. PloS One 2010;5:e9021.
24 Kiehn J, Karle C, Thomas D, Yao X, Brachmann J, Kübler W: HERG potassium channel activation is shifted by phorbol esters via protein kinase A-dependent pathways. J Biol Chem 1998;273:25285–25291.
25 Wang YH, Shi CX, Dong F, Sheng JW, Xu YF: Inhibition of the rapid component of the delayed rectifier potassium current in ventricular myocytes by angiotensin II via the AT1 receptor. Br J Pharmacol 2008;154:429–439.
26 Wang S, Xu D-J, Cai J-B, Huang Y-Z, Zou J-G, Cao K-J: Rapid component I(Kr) of cardiac delayed rectifier potassium currents in guinea-pig is inhibited by alpha(1)-adrenoreceptor activation via protein kinase A and protein kinase C-dependent pathways. Eur J Pharmacol 2009;608:1–6.
27 Thomas D, Wu K, Wimmer AB, Zitron E, Hammerling BC, Kathöfer S, Lueck S, Bloehs R, Kreye VA, Kiehn J, Katus HA, Schoels W, Karle CA: Activation of cardiac human ether-a-go-go related gene potassium currents is regulated by alpha(1A)-adrenoceptors. J Mol Med (Berl) 2004;82:826–837.
28 Hirdes W, Horowitz LF, Hille B: Muscarinic modulation of erg potassium current. J Physiol 2004;559:67–84.
29 McKay CM, Huizinga JD: Muscarinic regulation of ether-a-go-go-related gene K+ currents in interstitial cells of Cajal. J Pharmacol Exp Ther 2006;319:1112–1123.
30 Gentile S: Ion channel phosphorylopathy: a link between genomic variation and human disease. ChemMedChem 2012;7:1757–1761.
31 Schledermann W, Wulfsen I, Schwarz JR, Bauer CK: Modulation of rat erg1, erg2, erg3 and HERG K+ currents by thyrotropin-releasing hormone in anterior pituitary cells via the native signal cascade. J Physiol 2001;532:143–163.
32 Chen J, Chen K, Sroubek J, Wu ZY, Thomas D, Bian JS, McDonald TV: Post-transcriptional control of human ether-a-go-go-related gene potassium channel protein by alpha-adrenergic receptor stimulation. Mol Pharmacol 2010;78:186–197.
33 Barros F, Gomez-Varela D, Viloria CG, Palomero T, Giráldez T, de la Peña P: Modulation of human erg K+ channel gating by activation of a G protein-coupled receptor and protein kinase C. J Physiol 1998;511 (Pt 2):333–346.
34 Urrutia J, Alday A, Gallego M, Malagueta-Vieira LL, Aréchiga-Figueroa IA, Casis O, Sánchez-Chapula JA: Mechanisms of IhERG/IKr Modulation by α1-Adrenoceptors in HEK293 Cells and Cardiac Myocytes. Cell Physiol Biochem Int J Exp Cell Physiol Biochem Pharmacol 2016;40:1261–1273.
35 Radresa O, Guia A, Baroudi G: Roles of PKC Isoforms in PMA-Induced Modulation of the hERG Channel (Kv11.1). J Biomol Screen 2014;19:890–899.
36 Sugita S, Baxter DA, Byrne JH: Modulation of a cAMP/protein kinase A cascade by protein kinase C in sensory neurons of Aplysia. J Neurosci Off J Soc Neurosci 1997;17:7237–7244.
37 Gusovsky F, Gutkind JS: Selective effects of activation of protein kinase C isozymes on cyclic AMP accumulation. Mol Pharmacol 1991;39:124–129.
38 Tyanova S, Temu T, Carlson A, Sinitcyn P, Mann M, Cox J: Visualization of LC-MS/MS proteomics data in MaxQuant. Proteomics 2015;15:1453–1456.